Engineering Science and Technology, an International Journal 46 (2023) 101501

Contents lists available at ScienceDirect

Engineering Science and Technology, an International Journal

journal homepage: www.elsevier.com/locate/jestch

Influence of various fibers on the physico-mechanical properties of a sustainable geopolymer mortar-based on metakaolin and slag

Mahmoud Ziada [a], Savaş Erdem [b,*], Roberto Alonso González-Lezcano [c], Yosra Tammam [d], İrem Unkar [b]

[a] Civil Engineering Department, Faculty of Engineering, Istanbul Aydin University, Istanbul, Turkey
[b] School of Civil Engineering, Istanbul University - Cerrahpasa, Avcilar Campus, 34200 Istanbul, Turkey
[c] Architecture and Design Department, Escuela Politécnica Superior, Universidad CEU San Pablo, 28040 Madrid, Spain
[d] Istanbul Gelisim University, Civil Engineering Department, Avcilar Campus, Istanbul, Turkey

ARTICLE INFO

Keywords:
Geopolymer
Metakaolin
Slag
Fiber
High temperature
Sustainability

ABSTRACT

Recently, studies on sustainability and ecology have become widespread in almost all sectors. One of the most important reasons for this spread is the rapid increase in industrialization and, thus, the increase in waste caused by industries. In this context, significant efforts are being made to evaluate some of these wastes. One of these efforts is the production of geopolymers. In this research, metakaolin and slag-based geopolymer mortar samples were manufactured, and polyvinyl Alcohol, basalt, and macro synthetic polypropylene fibers were used to enhance the physical, mechanical, and high-temperature resistance of the sample. Physical and mechanical tests of the produced samples were performed after 28 days. Then, elevated-temperature experiments were conducted to evaluate the behavior of the fibers under the influence of high temperature. Following the high-temperature test, physical, mechanical and microstructure tests of the samples were performed. As a result, basalt fiber enhanced the compressive strength of 800 °C-exposed samples by 7.72% compared to the fiber-free sample. Also, polyvinyl Alcohol fiber increased the energy absorption capacity of the samples by increasing Charpy impact values to 72.22% compared to fiber-free sample. Moreover, macro synthetic polypropylene fiber reduced capillary water absorption value up to 12.44% compared to fiber-free sample.

1. Introduction

Cement consumption should be reduced in order to decrease global warming since it is necessary to decreasing the atmospheric emission of carbon dioxide [1]. Due to their low carbon footprint, geopolymer materials are a viable alternative to Portland cement materials [2,3]. Geopolymers are obtained by activating materials containing silica and alumina, like metakaolin, slag, fly ash, and red mud wastes, with alkalis such as KOH, NaOH, and Na_2SiO_3 [4]. A previous study [5] employed thermal treatment at temperatures ranging from 600 to 850 °C to transform kaolin into the amorphous and highly reactive metakaolin. They used thermokinetics and instrumental analysis to explore the heat transition of kaolin to metakaolin. Moreover, Geopolymer may be split into two types depending on the kind of activator, namely acid-based and alkali-based geopolymers, which emerge from activation in acid (humic acid and phosphoric acid) and alkaline environments, respectively [6,7]. Oxalic, sulfuric, phosphoric, and phosphate acids are utilized to make acid-activated geopolymers, but PA is the most common [8–11]. On the other hand, there are many studies have been focused on alkali solutions in geopolymers [12–16].

Previous studies [17–21] showed that the geopolymer is more resistant to chemical attack and weather conditions such as freezing and thawing than ordinary Portland cement (OPC). Sagoe-Crentsil et al. [22] demonstrate that geopolymer has reduced drying shrinkage than OPC concrete. Hu et al. [23], studied geopolymer's adhesion and abrasion resistance. Owing to its superior bonding ability and abrasion resistance, the findings demonstrated that geopolymer was superior to cement-based repair material. Owing to their ceramic-like microstructures and characteristics, geopolymers have excellent thermal-physical and mechanical capabilities when exposed to extreme temperatures, as is commonly accepted. Numerous investigations have been conducted on the characteristics of geopolymers at elevated temperatures, including thermal stability and physical and chemical features [24,25]. Jiang et al. [26] studied the physico-mechanical characteristics of a geopolymer

* Corresponding author.
E-mail address: savas.erdem@iuc.edu.tr (S. Erdem).

https://doi.org/10.1016/j.jestch.2023.101501
Received 12 March 2023; Received in revised form 16 July 2023; Accepted 29 July 2023
Available online 16 August 2023

manufacture with fly ash and waste glass powder, which was exposed to the consequence of elevated temperatures. In their study, it was found that the waste glass powder melted when it was exposed to high temperatures. Then the melted waste glass powder filled the pores of the geopolymer specimens. In this manner, they found that making use of glass powder waste in fly ash-based geopolymers could improve their resistance to high temperatures. Sakkas et al. [27] investigated the performance of geopolymers under a series of severe heat loads. The results showed that the geopolymer specimens retained structural integrity after being exposed to 800 °C, demonstrating the thermal barrier capability of this aluminosilicate material. Khater ve Gharieb [28] investigated the influence of nano-silica fume on improving the physical and mechanical characteristics and thermal behavior of MK-geopolymer composites. They found that incorporating 5% nano-silica fume into the MK geopolymer binder improved the physical and mechanical characteristics following exposure to high temperatures, in terms of strength. Alkaline-activated geopolymer based on metakaolin has gained popularity [29] because of its strong mechanical qualities comparable to cement, as well as its outstanding thermal stability. The most important source of metakaolin is kaolin, also known as kaolinitic clay or clay stone, from which it is continually possible to produce metakaolin by burning. The quality of metakaolin is determined by temperature, burning period, quantity burnt, and granule size [30,31]. Numerous investigations have demonstrated that the Metakaolin-based geopolymer covering has high fire resistance at 800 °C [32,33].

Flexible fibers have a deflection hardening behavior [34] that bridges over fractures created under stress, increasing the material's strength. The drying shrinkage is reduced because of the fiber-bridging action. Even more so, these fibers melt in a fire, creating channels for water vapor to escape. By doing so, the internal vapor pressure of the composites will be reduced, hence reducing the likelihood of cracking and eventual disintegration [35]. Recently, studies [36–39] have examined fibers that can improve composites' physical and mechanical properties, such as geopolymer. Research on geopolymer concrete by Rickard et al. [40] contrasted the high-temperature behavior during the hot stage with the residual values. Unlike cement concrete, they reported stronger residual compressive strength at temperatures up to 500 °C. The strength values for alkaline-activated materials including blends of slag and fly ash were established in experiments published by Pan et al. [41]. The found that the differences in strength between 300 and 600 °C imply significant variations in the bonding structures of these materials. Previous study [42] found that the dehydroxylation of the OH groups occur at higher temperatures (100–300 °C) due to evaporation of the chemically bound water. Lightweight aggregate concrete, geopolymer mortars, and pastes were tested by Abdulkareem et al. [43]. They found that the dehydration and dehydroxylation caused the 400–600 °C strength reduction. At 800 °C, geopolymer paste specimens lost all strength, but geopolymer mortar and lightweight concrete retained 50% and 60%, respectively. It was shown that aggregate type and qualities affected temperature resistance.

Due to the abundance of basalt (volcanic) rocks, which occupy approximately 70% of the earth's surface, basalt fibers (BS) are regarded as one of the most sustainable reinforcing fibers [44]. In addition, they have superior properties like high tensile strength, non-toxicity, durability, excellent corrosion resistance, and low production costs [45–47]. Previous research showed that when utilized at a precise dose, BS may improve the mechanical properties of the composites [48,49]. According to recent research, macro synthetic polypropylene (MSP) fibers reduce the corrosive behavior of structural parts and improve surface appearance [50,51]. Also previous studies [52,53] shown that the use of MSP fibers improves the mechanical properties of concrete.

Dhasindrakrishna et al. [54] investigated the rheology and high-temperature behavior of geopolymer foam concrete with various amounts of polyvinyl Alcohol (PVA) fiber. They found that the PVA fiber boosted the compressive strength of the hardened geopolymer foam concrete by up to 54% at a 3% dose. Additionally, the fire performance was enhanced regarding fire residual strength. They concluded that the enhancement was more noticeable at temperatures up to 200 °C. Haddaji et al. [55] investigated the flexural strength and microstructure of phosphate sludge-based geopolymers reinforced with glass fibers at high temperatures. They put forward that the flexural strength of phosphate sludge-based geopolymer matrix dropped between 25 and 600 °C but grew gradually at elevated temperatures, reaching an increase of 3.2% at 1000 °C. Zhang et al. [56] studied the behavior of fly ash and metakaolin-based geopolymer containing PVA fiber at high temperatures. They found that the inclusion of PVA fibers in a geopolymer mortar enhanced its flexural strength by 66.3%, its cubical compressive strength by 50.5%, and its prismatic compressive strength by 29.4% after being heated to 200 °C. Even though some PVA fiber disintegrated at temperatures over 200 °C, the flaws left by the melt fibers had a little impact on the mechanical properties of the geopolymer mortar samples. However, there is a dearth of research on the impacts of fibers on high temperature resistance of geopolymer mortars, particularly that also investigates the fibers' effects on capillary water absorption and energy absorption.

The improvement of some physical and mechanical properties of geopolymer mortars has always been a matter of curiosity for researchers. So, this paper has shown which fiber can achieve which property improvement by using 3 different fibers. Consequently, the primary objective of this research was to develop eco-friendly geopolymer mortars whose water permeability decreased and resistance to deformation and high temperatures enhanced. Therefore, this work produced samples of geopolymer mortar based on metakaolin and slag. In addition, PVA, BS, and MSP fibers were utilized in the geopolymer mortar samples at percentages of 0%, 0.5%, 0.75%, and 1% for enhancing the crack resistance behavior of geopolymer composites and make their application sustainable in load-bearing systems. Also, the capillary water absorption, Charpy impact, and compressive and flexural strength tests were carried on the 28-day specimens to evaluate their mechanical and physical properties. Also, visual inspection, mechanical tests, and Scanning Electron Microscopy (SEM) analyzes of the samples were conducted to evaluate the impact of 200, 400, 600, and 800 °C temperatures on the fiber-containing and non-fiber geopolymer samples.

2. Experimental work

2.1. Materials

This study used metakaolin (MK) and slag (S) as binder materials for geopolymer mortar samples. The chemical compositions of binder materials are given in Table 1. The specific gravities of metakaolin and slag materials used in geopolymer mortars were 2.52 and 2.90 g/cm^3, respectively. In addition, the chemical properties of Sodium hydroxide (NaOH) and sodium silicate (Na_2SiO3) materials used as activators of geopolymer mortar samples are given in Tables 2 and 3, respectively. In addition, the effects of PVA, BS, and MSP with various ratios on the physical, mechanical, and high-temperature resistance of the geopolymer mortars were investigated. These fibers were used by volume at 0.5, 0.75, and 1% ratios. Hence, the properties of these fibers are given in Table 4. Also, metakaolin, slag, sand, PVA, BS, and MSP used in fiber-containing metakaolin, and slag-based geopolymer mortar samples are shown in Fig. 1.

2.2. Mixture proportions and mixing procedures

This study produced metakaolin and slag-based geopolymer mortar samples using various fibers at different ratios. Besides the fiber-containing samples, fiber-free samples (0 F) were produced as control samples as shown in Table 5. The weights of materials were weighed with a precision balance before starting the mixing process. In addition, 12 molarity sodium hydroxide solution was made 24 h before the

Table 1
Chemical properties of MK and S (%).

Materials	Al_2O_3	SiO_2	CaO	TiO_2	Fe_2O_3	Na_2O	K_2O	MgO	Loss of Ignition
MK	40.23	56.1	0.19	0.55	0.85	0.24	0.51	0.16	1.1
S	12.83	40.55	35.58	–	1.1	0.79	–	5.87	0.03

Table 2
The chemical composition of Na₂SiO3 (%).

SiO_2	Na_2O	Fe	Density (g/ml) 20 °C	Heavy metals
26.5	9.60	≤0.005	1.36	≤0.005

Table 3
The chemical composition of NaOH (%).

NaOH	Na_2CO_3	Fe (%)	Al (%)	SO_4 (%)	Cl (%)
99	0.4	≤0.002	≤0.002	≤0.01	≤0.01

Table 4
The properties of PVA, BS, and MSP fibers*.

Fiber	Specific gravity	Melting temperature (°C)	Elasticity Module (GPa)	Length (mm)	Color
PVA	–	190–200	–	12	White
BS	2.73	–	88	12	Brown
MSP	0.91	165	10	12	White

*Provided by supplier of the fibers, the company Arkem Chemical in Istanbul, Turkey.

blending process and left to cool. Then, Na₂SiO3 solution was added to the obtained NaOH solution in a 1:2 ratio. Thus, the activator solution was obtained and mixed homogeneously with metakaolin. Afterward, slag was added and blended homogeneously for 2 min. Then, the sand and fibers at 0, 0.5, 0.75, and 1% volume ratios were added to the mixtures and mixed homogeneously for 2 min. Finally, the obtained mixtures were poured into 40x40x160mm and 50x50x50mm molds, pre-lubricated, placed on a vibration table, and vibrated. After one day, the hardened samples were taken off their molds and kept at 20 ± 2 °C for 28 days.

2.3. Tests conducted

In this study, various fibers were added to the geopolymer mortar specimens with different percentages to investigate how fibers affect the mechanical and physical characteristics of the geopolymer mortar. Thus, capillary water absorption, compressive strength, Charpy impact, and flexural strength experiment were conducted to look at the impact of

Table 5
Mixture proportions of metakaolin and slag-based geopolymer series (kg/m^3).

Series	MK	S	NaOH	Na₂SiO3	Sand	Fiber Vol (%)
0 F	310	276	158	316	1140.5	0.00
0.5 PVA	310	276	158	316	1140.5	0.50
0.75 PVA	310	276	158	316	1140.5	0.75
1 PVA	310	276	158	316	1140.5	1.00
0.5 BS	310	276	158	316	1140.5	0.50
0.75 BS	310	276	158	316	1140.5	0.75
1 BS	310	276	158	316	1140.5	1.00
0.5 MSP	310	276	158	316	1140.5	0.50
0.75 MSP	310	276	158	316	1140.5	0.75
1 MSP	310	276	158	316	1140.5	1.00

Fig. 1. Images of materials and fibers used in geopolymer mortar blends: (a) Metakaolin, (b) slag, (c) sand, (d) PVA, (e) BS, and (f) MSP.

PVA, BS, and MSP content on the properties of the samples. Furthermore, SEM analyses of 1 PVA, 1 BS, and 1 MSP samples were performed. The specimens were then exposed to the elevated-temperature effect. The specimens that were subjected to high temperatures were performed to bending and compressive strength testing. Thus, the mechanical properties of the fibers before and after the impact of elevated temperatures were compared.

The fiber-free specimens and those containing PVA, BS, and MSP fibers with different ratios were stored for 28 days at 20 ± 2 °C. After 28 days, three 50x50x50 cube samples from each series were conducted to a compressive strength test using 2000 kN capacity press machine, and the average value of the obtained results was considered. The compressive strength tests were carried out according to ASTM C39 and with a speed of 0.6 MPa/sec. In addition, three 40x40x160 prism specimens from each series were conducted to a flexural strength test using 3-point bending test machine, and the average value of the obtained results was considered. The flexural strength tests performed in this research were conducted according to ASTM C 348.

Then, 40x40x160 prismatic geopolymer mortar samples were subjected to the Charpy impact test using pendulum impact Charpy test machine. According to ASTM E23, the Charpy impact test was applied, and it was compatible with the previous work performed by ZIADA et al. [14]. Hence, the experimental setup and procedure shown in Fig. 2 were used to conduct the Charpy impact test. The results of geopolymer samples containing fiber were compared with the results of geopolymer samples without fiber using the obtained results in kgf-m units. Thus, the increases in Charpy impact percentages of the fibrous specimen in comparison to the 0 F samples were determined.

The capacities of capillary water absorption of fibrous and fiber-free geopolymer mortar specimens were calculated according to ASTM C1585. In addition, a capillary water absorption test was performed similarly to previous studies' capillary water absorption experiments [14,57,58]. The tests of water absorption were conducted on 40x40x160 specimens. As the first step of this experiment, the samples were dried in the oven until they reached constant weight. Subsequently, the surfaces of the specimens were coated using paraffin, with the exception of the test surface. Then, the samples were placed on wooden sticks to sink in water at a depth of 5 mm. The samples kept in water were taken out of the water after 1, 3, 5, 24, 48, and 72 h. Subsequently, their weights were measured, and the weight differences were calculated by subtracting the difference from their initial weights. In addition, the capillary water absorption coefficient was calculated using the least squares method and formula 1, as in the study of Tanıyıldız et al. [57].

$$K_C \times \sqrt{t} = \frac{Q}{A} \quad (1)$$

Kc, capillary water absorption coefficient ((kg/ (m^2. $\sqrt{s}$))); t is time; Q, Weight difference (kg); A is the area of the submerged surface (m^2).

Moreover, fibrous and free-fiber geopolymer mortar specimens based on metakaolin, and slag were subjected to elevated-temperature effects. In the first stage of the experiments, the specimens were oven-dried until they reached a constant weight. Then, the high-temperature furnace was set to 5 °C per minute, and the dried samples were placed in it. Thus, as seen in Fig. 3, using high temperature furnace the high-temperature test was completed one hour after the temperature increased and reached 200, 400, 600, and 800 °C in four groups separately. In other words, the samples were placed in the furnace, and they were exposed to the increasing temperature until reaching temperatures 200, 400, 600, and 800 °C. Then, the samples were kept in the furnace for one more hour under the influence of the 200, 400, 600, and 800 °C separately. Following that, the samples were allowed to cool freely in the furnace. After 24 h, the samples cooled down. This heating rate adheres to RILEM guidelines to reduce strains caused by temperature variations between the sample's hotter surface and colder interior [59]. Subsequently, compressive and flexural strength tests were performed

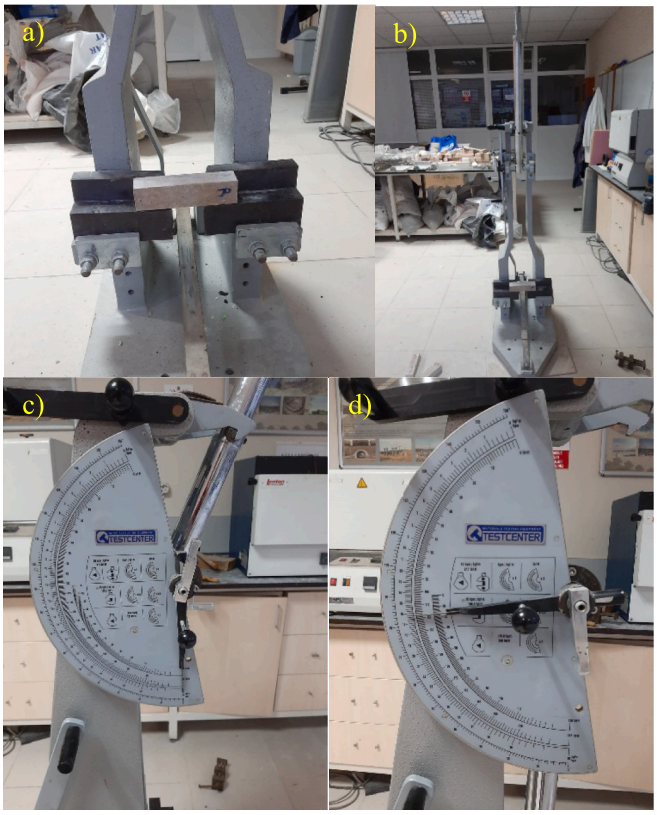

Fig. 2. Charpy impact test procedure: (a) Placing the sample in its assigned area, (b) Raising the pendulum of the device, (c) setting the drag indicator to zero, (d) getting values obtained on the drag indicator.

Fig. 3. Cube and prism geopolymer mortar samples placed in a high-temperature furnace.

on the specimens. Hence, flexural strength values of 40 × 40 × 160 mm prismatic specimens subjected to the elevated-temperature impact were found. Also, the compressive strengths of 50 × 50 × 50 mm cube specimens were performed. The visual inspections of the specimens subjected to elevated temperature and flexural tests were conducted. Finally, SEM analysis was performed using Zeiss EVO LS 10-SEM device to evaluate the microstructural of the samples in general and examination the fibers in the matrix.

3. Results and discussions

3.1. Compressive strength and flexural strength results

After 28 days, three 50x50x50 cube samples from each series were subjected to a compressive strength test, and the results were averaged. The compressive strength test's average results of 0 F, 0.5 PVA, 0.75PVA, 1 PVA, 0.5 BS, 0.75 BS, 1BS, 0.5 MSP, 0.75 MSP, and 1 MSP series are shown in Fig. 4. Generally, it was discovered in this work that increasing the fiber content in geopolymer mortar enhanced the compressive strength of the specimens. As illustrated in Fig. 4, according to 0 F samples, the compressive strength of 0.5 PVA, 0.75PVA, and 1 PVA increased by 1.81, 3.11, and 2.17, respectively. The compressive strength of metakaolin and slag-based geopolymer mortars increased marginally to 0.75% PVA fiber concentration, then decreased slightly by 1% PVA. The compressive strength increases of 0.5 PVA and 0.75 PVA samples was due to PVA preventing fracture development and carrying the load. In a previous study [60], the compressive strength of cementitious composites containing 0.3, 0.6, 0.9, 1.2, and 1.5% PVA fiber was investigated, and it was found that the compressive strength decreased after the PVA content was 0.6%. As stated by previous studies [61,62], excess PVA fiber created additional voids in the matrix, leading to a decrease in compressive strength. The increase in PVA content complicates the consolidation process of PVA in the matrix and thus leads to an increase in the porosity of the matrix [63].

Also, the compressive strength of 0.5 BS, 0.75 BS, and 1 BS increased by 1.06, 3.46, and 4.30%, relative to 0 F specimens. As a result, it was determined that the content of BS fiber enhanced the compressive strength of the metakaolin and slag-based geopolymer specimens. Katkhuda and Shatarat [64] examined the influence of BS fiber on the mechanical properties of concrete. They found that adding BS fiber improved the compressive strength of the concrete. Also, their study found the highest compressive strength with a BS fiber content of 1%. However, Niaki et al. [65] found that the addition of BS at a concentration of 0.5–3.5 wt% enhanced the compressive strength up to an optimal fiber content of 2%. At a fibers concentration of 2%, the compressive strength rose by approximately 10% in comparison with the control mixture. At 0.3 vol% of BS, Jiang et al. [66] recorded a maximal 10% improvement in compressive strength.

On the contrary, the increase of MSP fiber decreased the compressive strength of the geopolymer mortar samples. Consequently, the compressive strength of 0.5 MSP, 0.75 MSP, and 1 MSP decreased by 0.75, 1.06, and 1.96, respectively. Previous studies [67,68] have shown a reduction in the compressive strength of samples when different kinds of MSP fibers are added. This decrease may be ascribed to the presence of pores caused by the inclusion of MSP fibers and the presence of weak interfacial connections between the matrix and MSP fibers [69]. The pores and weak interfacial connections between the matrix and MSP fibers are caused because the fact that the surface of MSP fibers is hydrophobic, so they did not wet by the geopolymer mortar.

The average value of three 40x40x160 prism specimens from each series were tested for flexural strength. Fig. 5 illustrates the effect of flexural strength test results of geopolymer samples containing PVA, BS, and MSP fiber in various ratios. As seen in Fig. 5, the flexural strengths of all samples containing fiber were higher than the 0 F samples. In addition, the max rising in compressive strength reached 4.30%, while the max rising in flexural strength was found to be 14.05%. As showed in Fig. 5, the flexural strength results of 0.5 PVA, 0.75 PVA, and 1 PVA increased by 5.13, 11.18, and 14.05%, respectively, compared to 0 F samples. It demonstrates that the flexural strength improved dramatically when the PVA fiber concentration rose from 0% to 1%. Flexural strength increased fastest with a 1% PVA fiber concentration. This increase in flexural strength was attributed to the connection established by PVA fiber, which increased tensile zone strength [70]. A previous study [71] showed that PVA fibers with content between 2 and 3% sound to be the most efficient at enhancing the durability, and structural integrity of cementitious composite. Also, Akkari [72] stated that with a small fiber percentage of 0.77%, it was feasible to obtain the highest compressive strength and flexural strength in comparison to the other fiber ranges used. Additionally, the flexural strength of 0.5 BS, 0.75 BS, and 1 BS rose by 3.50, 8.68, and 10.98, respectively, compared to 0 F samples. Hence, the flexural strength of 1 PVA increased by 14.05% compared to the 0 F samples, while the flexural strength of BS increased by 10.98%. Thus, the PVA fiber enhanced the geopolymer mortar samples more effectively than the BS fiber. Consequently, it was found that adding BS fiber to metakaolin and slag-based geopolymer mortar samples increased their flexural strength values. Because BS fibers arresting the crack growth of the samples, they significantly decreased the cracks performed by the flexural tests. The fact that the fibers arrest and inhibit the crack growth is also valid for samples containing other fibers subjected to mechanical tests. Also, they slowed fracture

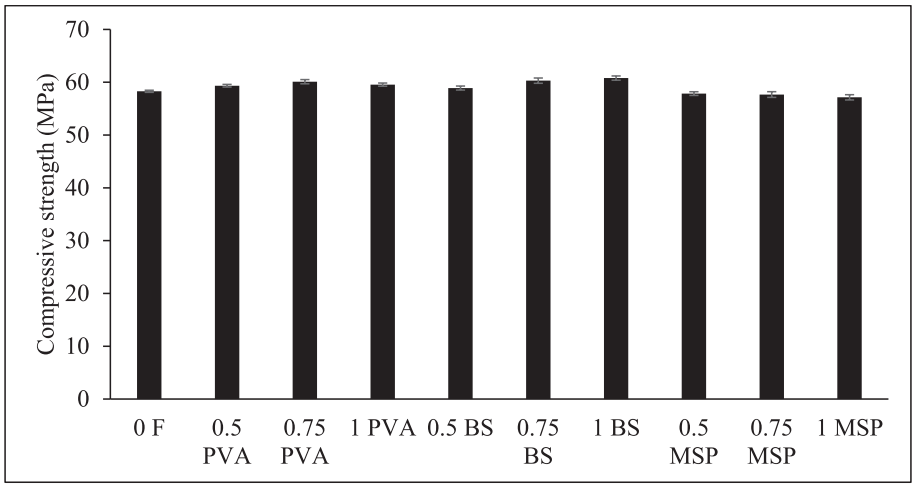

Fig. 4. Compressive strength test results of geopolymer mortar-based on metakaolin and slag contained PVA, BS, and MSP fiber in various ratios.

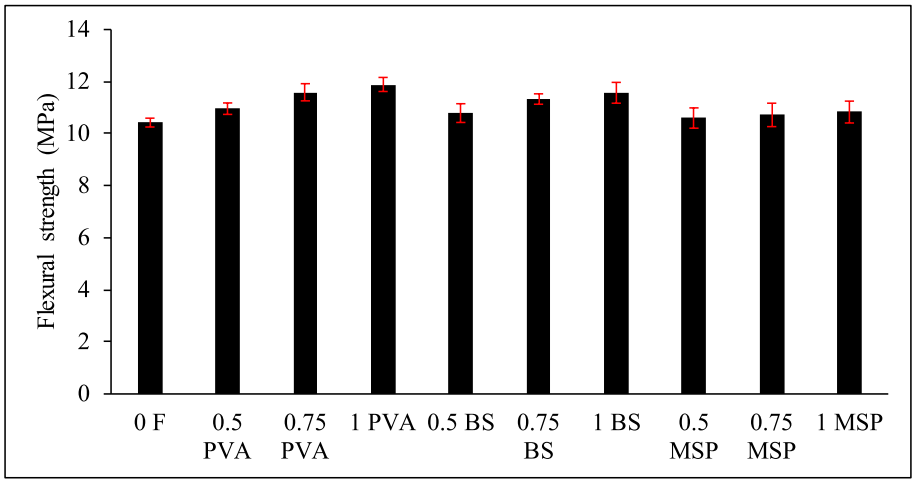

Fig. 5. Flexural strength test results of geopolymer samples contained PVA, BS, and MSP fiber in various ratios.

formation by dispersing the resulting tension. Consequently, BS fibers significantly increased flexural strength. These findings were consistent with previous studies [14,73]. Katkhuda and Shatarat [64] claimed that flexural strength increased continuously beyond 0.3% fiber content. The flexural rigidity of the fiber-reinforced concrete increased by approximately 75% relative to the normal concrete. Jiang et al. [66] observed that adding basalt fiber to concrete enhances its flexural strength. They also stated that the flexural strength increased with the number of basalt fibers. However, when the percentage of BS surpassed 0.3%, the flexural strength dropped in comparison to samples containing a lower percentage of basalt fibers. In addition, although the increase in MSP fiber decreased the compressive strength of the geopolymer mortar specimens, it increased the flexural strength of the same series. It was noted that the flexural strength values of 0.5 MSP, 0.75 MSP, and 1 MSP increased by 1.68, 2.83, and 3.88, respectively. This may be due to the bridging function of the fibers, which limits the fracture propagation and narrows cracks, as demonstrated in a previous study [74].

3.2. Charpy impact test results

This experiment was conducted on three 40x40x160 mm geopolymer prismatic samples based on metakaolin and slag for each series. Also, the average findings were obtained in kgf-m units. Then, percent increases of the performed results of the fiber-containing samples were calculated compared to the values of the fiber-free samples, and these increases are given in Fig. 6. The Charpy impact experiment test takes advantage of the potential energy of a falling pendulum to crack specimens at large strains and describe the composites. Mechanical characteristics evaluation depends on the propagation of stress waves, potential energy, or kinetic energy [75]. Consequently, including PVA, BS, and MSP fibers improved the Charpy impact experiment results of the samples. All series' Charpy impact experiment findings ranged between 16.2 and 27.9 kgf-m. The highest increases were seen in 1 PVA samples, about 72.22%, compared to 0 F samples. Impact energy absorption and analogous attributes rely significantly on fiber qualities [76]. Also, the energy absorption capacity of PVA fiber was emphasized in previous studies [39,77]. In addition, increasing the percentage of MSP fiber increased the Charpy impact test results. This can be attributed to the fact that the MSP fiber used in this study has ribbed-surface, which could help it to absorb more energy.

3.3. Capillary water absorption results

The 28 days geopolymer samples were exposed to capillary water absorption. The results of three samples for every series were found, and the average results of each series were determined. The curves of

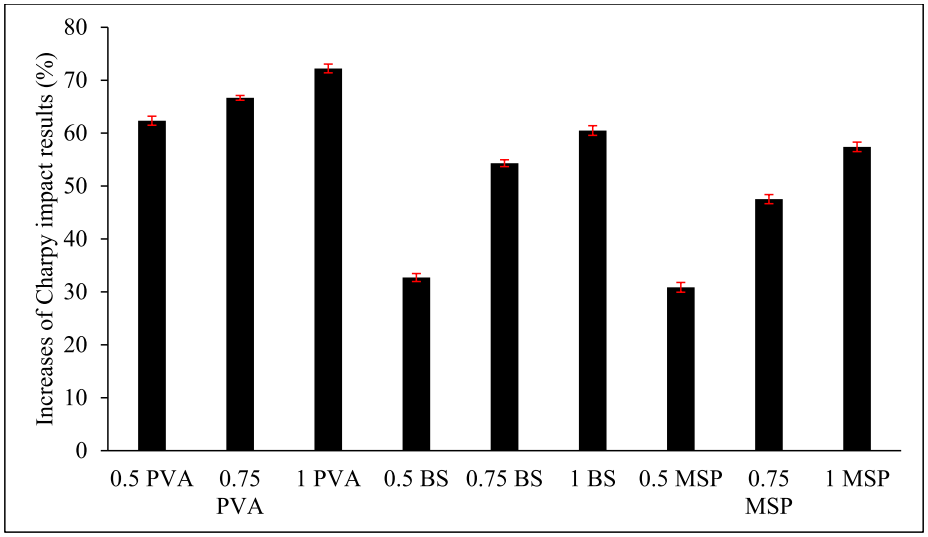

Fig. 6. Increases of Charpy impact results of geopolymer mortars contained fibers compared to 0 F sample.

capillary water absorption illustrated in Fig. 7 were created by measuring the quantity of absorbed water over time in terms of the water's contact area. As shown in Fig. 7, increasing the BS fiber and PVA fiber content increased the water absorption capacity of the samples, while increasing the MSP fiber content decreased the water absorption capacity of the samples. Fig. 8 illustrates the capillary water absorption coefficient (Kc) of the samples containing fibers and sample-free fiber (0 F). The least-squares method was utilized to obtain Kc values. Kc of 0.5 PVA, 0.75 PVA, and 1 PVA increased by 0.40, 2.84, and 5.39%, respectively, compared to 0 F samples.

The water absorption capacity of fiber-contained matrix is highly reliant on the composites' transition zone thickness and porosity. The inclusion of fiber can enhance the thickness of the transition zone and the porosity of the transition zone, hence increasing water absorption [78]. Similarly, a previous study [79] indicated that the inclusion of PVA fibers increased the water absorption capacity of geopolymer specimens.

Also, water absorption coefficients of samples 0.5 BS, 0.75 BS, and 1 BS increased by 2.77, 5.41, and 9.54%, relative to 0 F specimens. These increases occur due to the inclusion of basalt fibers, which enhances of connectivity of pores at fractions. Comparable outcomes were reported in previous studies [14,80,81]. In contrast, water absorption coefficients of samples 0.5 MSP, 0.75 MSP, and 1 MSP decreased by 7.16, 8.26, and 12.44%, respectively, compared to 0 F samples. Because of the fact that the surface of MSP fibers is hydrophobic, the MSP fiber-contained samples absorbed less water than PVA and BS fibers-contained samples. Behfarnia and Behravan [82] investigated polypropylene fibers' performance in concrete and found that water absorption decreased in all fiber-containing concrete examples. Also, Bolat et al. [83] investigated the performance of macro synthetic fibers in concrete, and they found that the synthetic fiber content decreases the capillary water absorption of the concrete samples. In addition, Saradar et al. [84] found that BS dosage enhances concrete water absorption. Dilbas and Cakir's [85] investigation on BS dose and concrete water absorption yielded similar results.

3.4. Visual assessment after high-temperature tests

In order to investigate the effect of high temperature on the fibrous and non-fiber geopolymer mortar samples, the images of the middle sections of the samples were observed and shown in Table 6. For this purpose, 0 F, 1 PVA, 1 BS, and 1 MSP samples exposed to 20, 200, 400, 600, and 800 °C temperatures were examined. As Table 6 shows, when

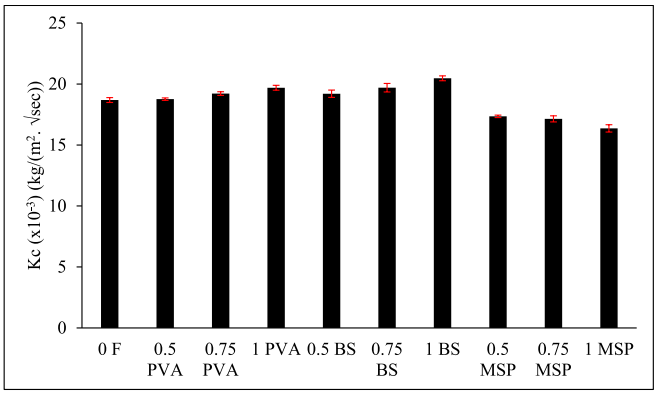

Fig. 8. Kc of geopolymer samples contained various ratios of PVA, BS, and MSP fiber.

the temperature to which 1 PVA sample is exposed changes from 20 °C to 200 °C, the color of the PVA fibers changes from white to brown. Also, after 400 °C, the PVA fibers disappeared. This result was consistent with a previous study [54]. This study also observed that the fibers partially melted when the temperature to which 1 MSP samples were exposed changed from 20 °C to 200 °C, and after 400 °C, the MSP fibers melted completely. Also, when the MSP fibers melted, caused pores and channels formed instead as shown in Table 6. In addition, as seen in previous studies [86], the inside color of the specimens started to darken at 400 °C, and it was observed that it turned gray until it reached 800 °C. Although MSP melt at 165 °C and PVA melt at 190–200 °C (Table 4), and they melt completely when exposed to 400 °C while they are in the geopolymer matrix (Table 6), BS fiber is more resistant to higher temperatures relatively. Because of this, the samples containing 3 different fibers were exposed to temperatures between 200 and 800 °C to do an accurate comparison among the 3 fibers. Thus, the damages left in place by the molten fiber were examined. For instance, according to visual assessment and the mechanical tests carried out in the study, when the MSP fibers melted, the gaps and channels left behind were larger and the damage was more than PVA fibers.

3.5. Compressive and flexural strength after high-temperature tests

The effect of PVA, BS, and MSP fibers on the mechanical properties of

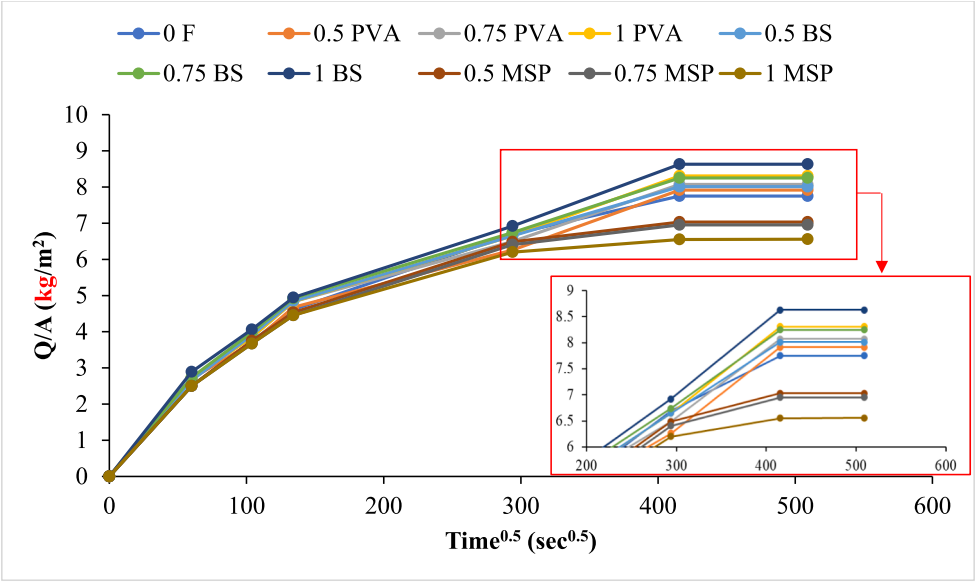

Fig. 7. Capillary water absorption curves of geopolymer samples contained PVA, BS, and MSP fiber in various ratios.

Table 6
Images of fibrous and non-fiber geopolymer specimens subjected to high-temperature effects.

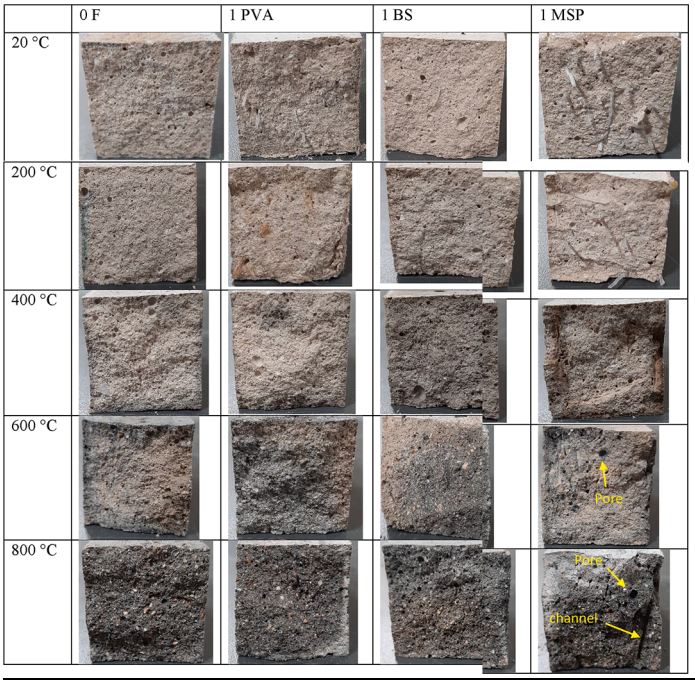

geopolymer mortar samples exposed to high-temperature effects was investigated. Hence, flexural and compressive strength values of the specimens exposed to high-temperature effects were obtained. The average results for each series were determined based on the results of three samples for each series. Figs. 9 and 10 illustrate the compressive and flexural strength values of high-temperature exposed metakaolin and slag-based geopolymer mortar samples. It was observed that the compressive strength of the 0 F sample increased by 6.18% when the temperature increased by 200 °C. Also, it was noticed that the sample's bending strength increased by 1.68% when the temperature of the 0 F sample was increased to 200 °C. The reason for this is that the unreacted particles in the metakaolin and slag-based geopolymer mortar samples reacted with the temperature effect, and this caused the samples to be more compact [87]. However, the same is not valid for all fiber-containing samples. For example, the increase in PVA content of samples containing PVA from 0.5% to 1% decreased the compressive strength increases from 3.13% to 0.84. In addition, the increase in PVA content of the samples containing PVA decreased the flexural strength increases from 2.16% to 1%. Previous investigations demonstrated that fibrous geopolymer concrete provides superior bond strength relative to OPC concrete [88,89]. According to previous studies [90,91], the addition of various fibers is recommended to enhance the mechanical bond of the concrete matrix. However, in this study, increasing temperature causes deformation and melting of PVA and MSP fibers. Therefore, it is thought that as the fibers melt, their mechanical bond with the matrix decreases.

Conversely, it was for samples containing BS. As a result, the samples' compressive strength rose from 3.98% to 4.31% due to the increase in BS percentage. Additionally, the samples' higher BS content caused a rise in flexural strength from 5.92% to 9.64%. The reason for this is that BS fibers are not affected by 200 °C. The opposite hand, the compressive strength of the MSP fiber specimen's exposure to 200 °C declined

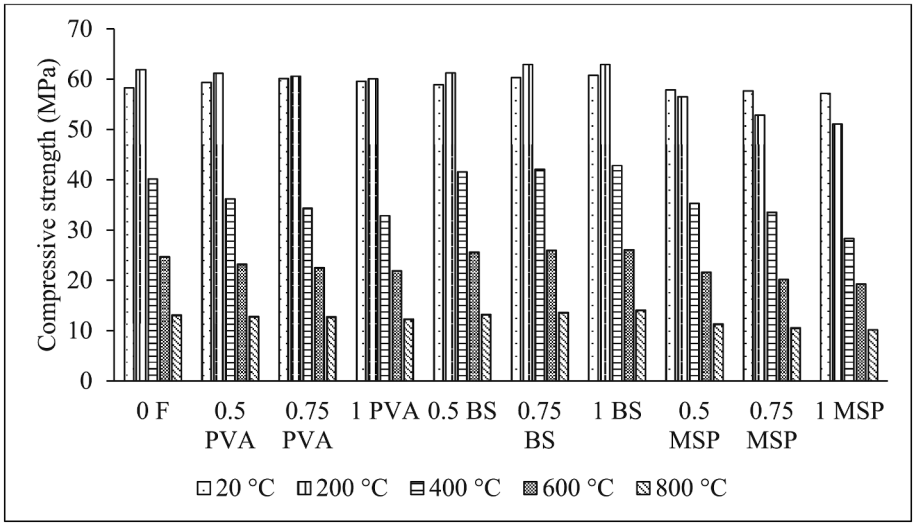

Fig. 9. Compressive strength results of geopolymer samples subjected to the elevated-temperature effects.

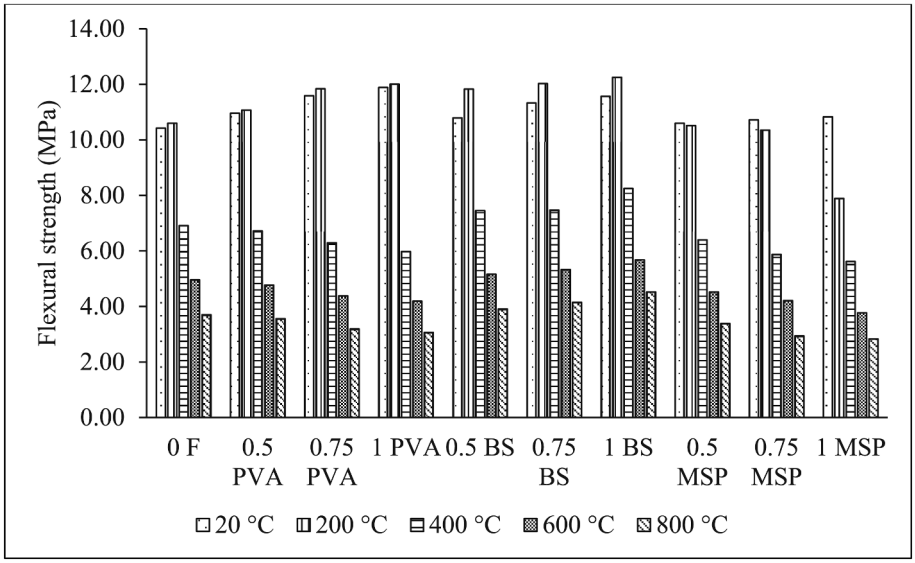

Fig. 10. Flexural strength results of geopolymer samples subjected to the elevated-temperature effects.

relative to the 20 °C specimens, unlike the PVA and BS specimens. A previous study [92] analyzed the efficiency of using BS to resist high temperatures and found that concrete containing BS may be utilized at high temperatures (200–800 °C). However, these decreases increased when the fiber content rises. This is due to MSP fibers' high-temperature sensitivity and low melting point. Therefore, when the samples' MSP

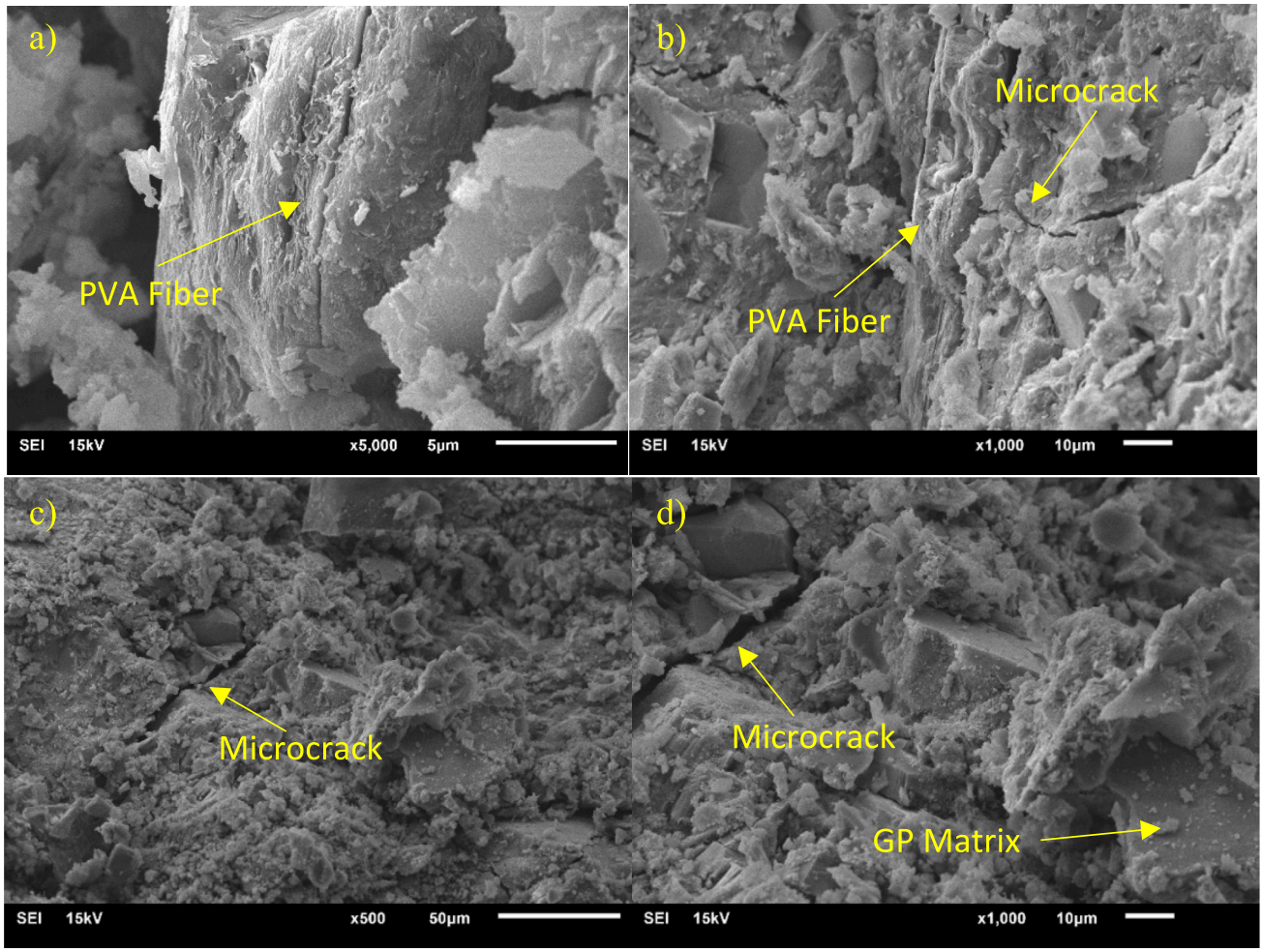

Fig. 11. (a, b) 500× and 1000× magnified SEM images of 200 °C exposed 1 PVA samples (c, d) 500× and 1000× magnified SEM images of 400 °C exposed 1 PVA samples.

percentage rose, the compressive strength drops from 2.33% to 10.68%. In addition, the increase in MSP content in the samples increased the flexural strength decreases from 0.85% to 27.15 %.

After 400 °C, the compressive strength decline of PVA and MSP samples started to be more pronounced and continued up to 800 °C, contrary to the samples containing BS fiber. In comparison to the 0 F specimens, the specimens with PVA fiber exposed to 800 °C decreased by 5.95%, and the samples with MSP fiber decreased by 22.54%. In contrast, the samples with BS fiber increased by 7.72% compared to the 0 F sample. In addition, the highest compressive strength drops of the samples with PVA, BS, and MSP fiber were obtained as 82.25% from 1 MSP sample relative to the 20 °C samples. In addition, the bending strength decreased increased from 1% to 74% compared to the 20 °C samples. These reductions were thought to be due to endothermic processes and the occurrence of dehydration in the matrix [86]. While the water particles in the samples evaporated, the steam movement negatively affected the sample's internal structure. In addition, the alumina-silica gel crystallized with the increase in high temperature, which caused the voids in the matrix to increase [93]. In addition, in the previous study [94], it was emphasized that the increase in high temperature caused the formation of microcracks in the matrix's interfacial transition zone (ITZ), and thus thermal mismatches occurred.

3.6. SEM analyses

SEM analysis of geopolymer mortar samples based on metakaolin and slag subjected to elevated-temperature effect was conducted. Because PVA and MSP fibers has melting point close to 200 °C, SEM images were obtained when 1 PVA, 1 BS, and 1 MSP specimens were subjected to 200 °C and 400 °C. In addition, SEM analysis of the 0 F sample subjected to the same temperatures was also performed for comparison. Thus, SEM analyses of 1 PVA, 1 BS, 1 MSP, and 0 F specimens subjected to 200 and 400 °C are given in Figs. 11-14, respectively. In Figs. 11-14, (a) and (c) coded images were magnified at 500x; however, (b) and (d) coded images were magnified at 1000x. Fig. 11(a) and (b) illustrate the PVA fiber in the matrix in 1 PVA sample exposed to 200 °C. Moreover, the inhibition of microcrack expansion formed by PVA fiber is shown especially in Fig. 11(b). On the other hand, in 1 PVA sample exposed to 400 °C in Fig. 11(c), it was seen that the PVA fiber was not seen in the matrix; thus, there was no obstacle to the development of microcracks. Fig. 12 (a) and (b), showing 1 BS sample and 1 PVA sample, show the BS fiber in the matrix when subjected to 200 °C. Also, 1 PVA sample subjected to 400 °C in Fig. 11 did not contain PVA, while Fig. 12 (c) and (d) showed the presence of BS in 1 BS sample exposed to 400 °C. Hence, the resistance of BS to 400 °C demonstrated in previous tests was consistent with SEM analysis. This was also because the fact

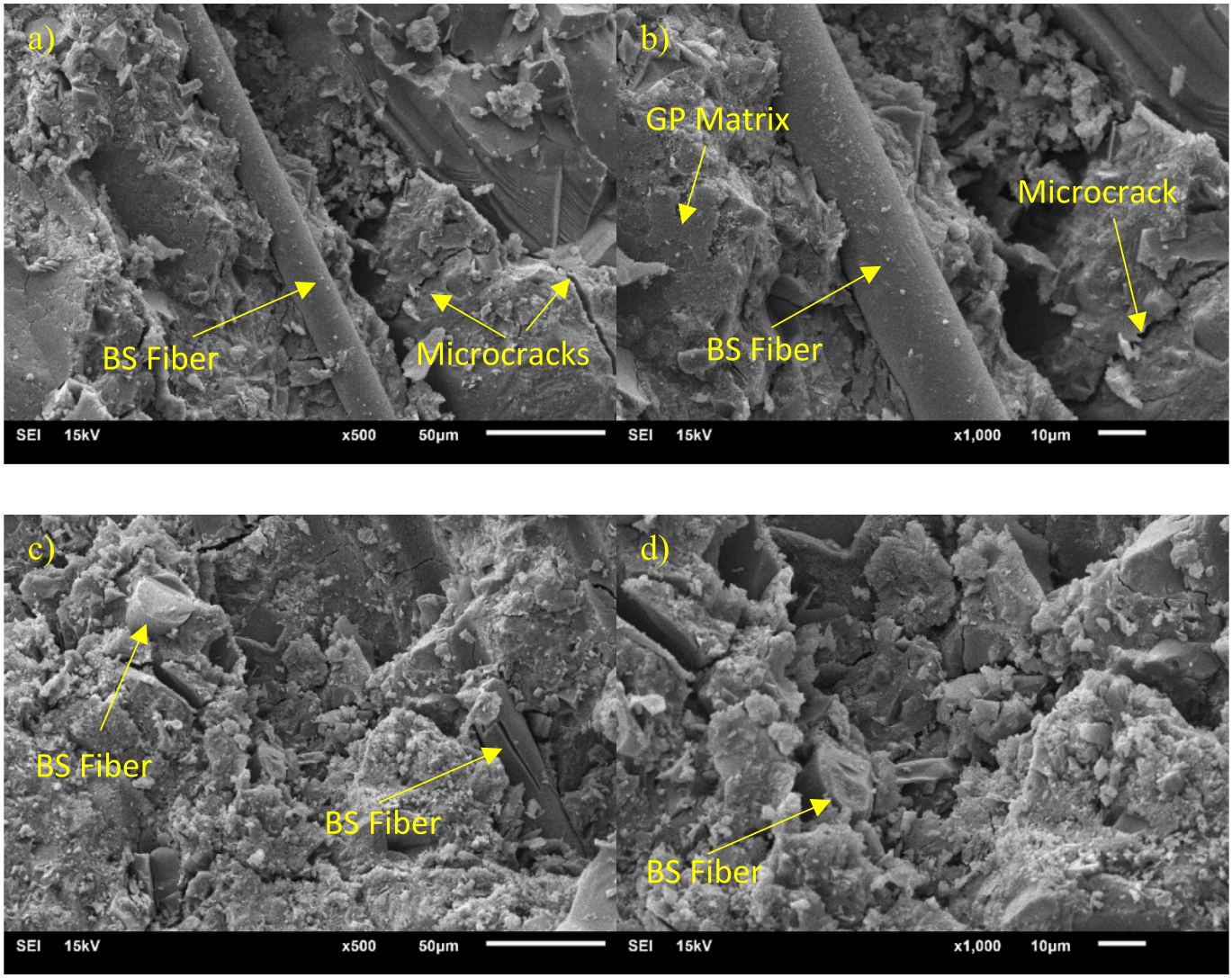

Fig. 12. (a, b) 500× and 1000× magnified SEM images of 200 °C exposed 1 BS samples (c, d) 500× and 1000× magnified SEM images of 400 °C exposed 1 BS samples.

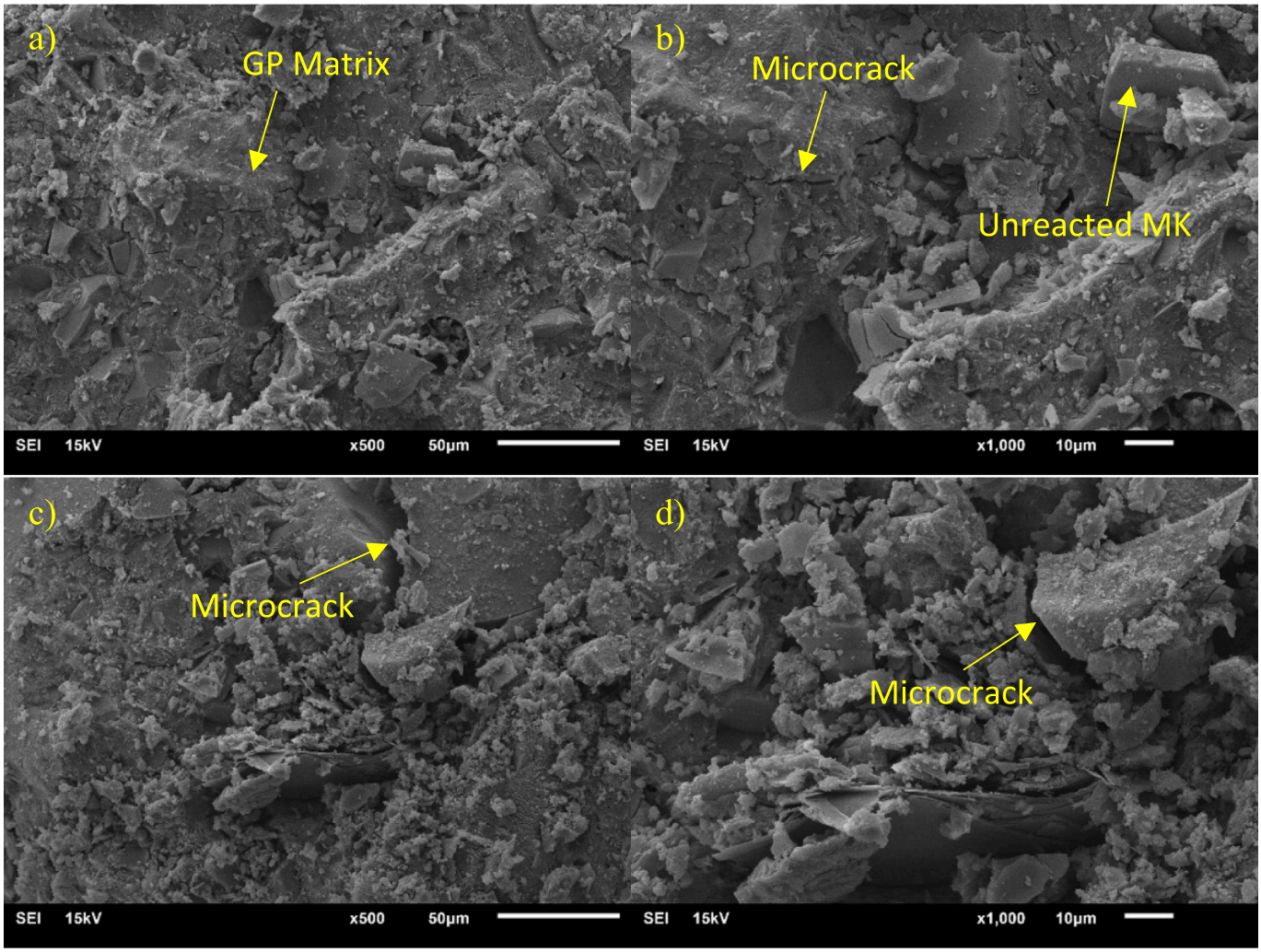

Fig. 13. (a, b) 500× and 1000× magnified SEM images of 200 °C exposed 1 MSP samples (c, d) 500× and 1000× magnified SEM images of 400 °C exposed 1 MSP samples.

that the BS fiber slowed the expansion movement of cracks [14,95]. In addition, Fig. 12 (c) shown the surface of the fibers has notches. This could be attributed to the effects of alkalis on BS. Furthermore, some matrix particles can be seen on the surface of the pull-out BS fibres indicating that BS fibres were closely bonded with the surrounded geopolymer matrix. Afroz et al. [96] examined the influence of the principal compounds responsible for concrete deterioration such as sulfate, chloride, and alkalis on Bs. The fibers were unaffected by chloride and sulfate solutions, but they were affected by alkali solutions. On the other hand, the 1 MSP samples shown in Fig. 13 had a more irregular and hollow interior structure than the other samples. In addition, the presence of foreign particles in the 1MSP sample exposed to 400 °C could be attributed to the fact that the MSP fibers completely dissolved and changed their shape. Finally, Fig. 14 (a) and (b) show that the 0 F sample exposed to 200 °C had a continuous geopolymer matrix and a more compact structure than the 1MSP sample. However, it was observed that the 0 F sample contained more microcracks than the 1 BS sample when exposed to 400 °C. This was because of the increase in the rate and amount of water loss due to the evaporation of water particles in the samples exposed to 400 °C, and this caused the cracks to be formed. Thus, cracks and voids formed in the samples caused the internal structure of the samples to deteriorate [43].

4. Conclusion

This study produced metakaolin and slag-based fibrous geopolymer mortar samples using PVA, BS, and MSP fibers. After comparing and analyzing the obtained results of this study, the findings are summarized below:

1. Compared to the 0 F samples, the compressive strengths of the specimens containing PVA and BS increased, On the contrary, using MSP fiber reduced the compressive strength of the geopolymer mortar samples. Also, the flexural strengths of all fiber-containing specimens were bigger than the 0 F specimens. Including PVA, BS, and MSP fibers improved the Charpy impact test results of metakaolin and slag-based geopolymer samples. Thus, the PVA fiber samples had more energy absorption than the other fibers; thus, the impact of energy absorption significantly depended on the fiber used.
2. The color of PVA fiber in geopolymer mortar specimens subjected to 200 °C turned brown, and PVA fibers burned after 400 °C. Similarly, MSP fibers in geopolymer samples exposed to 400 °C completely melted, and pores were formed instead. Also, the inner color of the specimens subjected to 800 °C turned gray. Eventually, while the flexural and compressive strength of the specimens containing PVA and BS fibers was subjected to 200 °C relatives to the specimens at 20 °C, the flexural and compressive strength of specimens containing MSP fiber decreased. In addition, after 400 °C, the flexural and

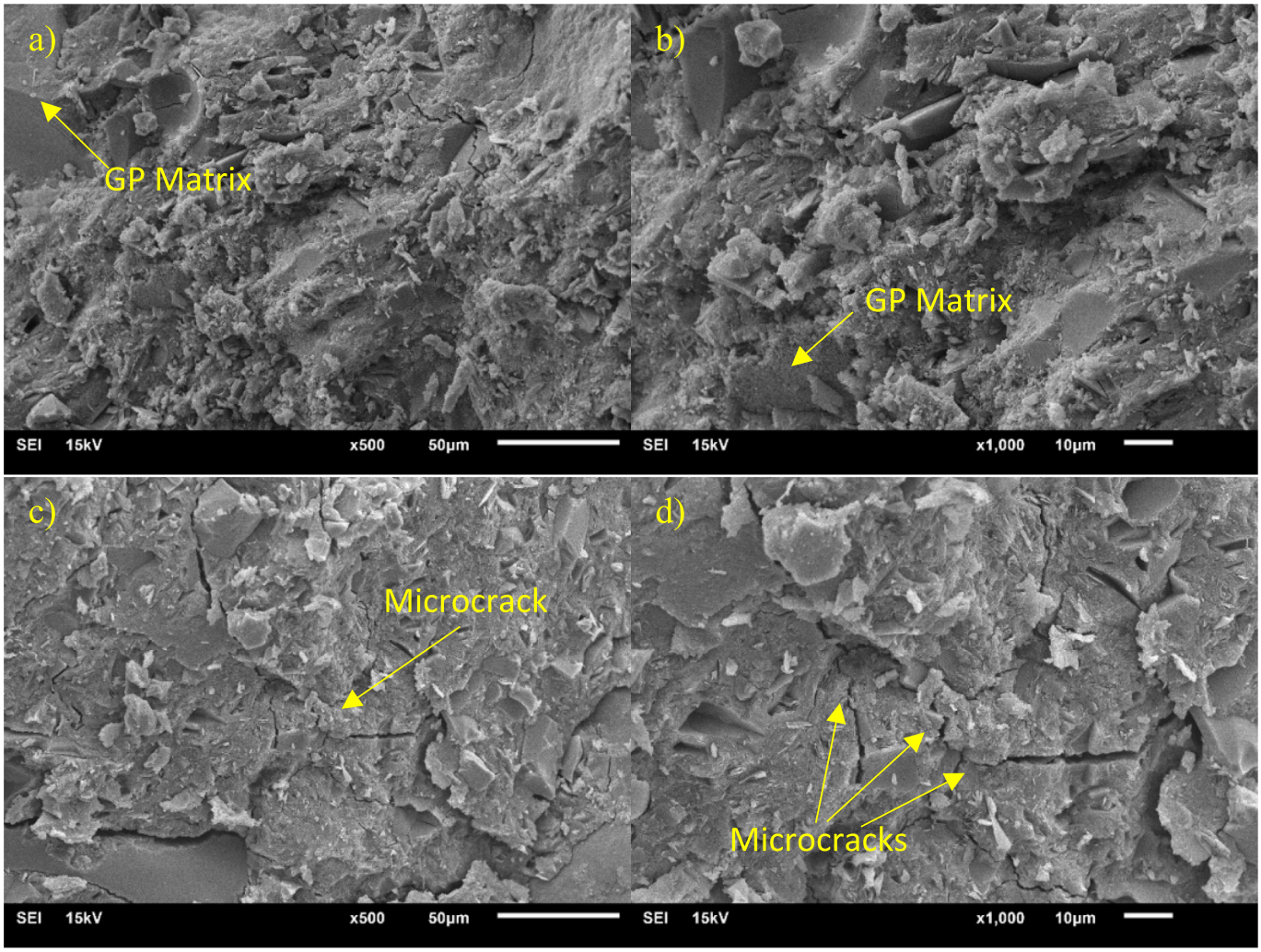

Fig. 14. (a, b) 500× and 1000× magnified SEM images of 200 °C exposed 0 F samples (c, d) 500× and 1000× magnified SEM images of 400 °C exposed 0 F samples.

compressive strength drops of the specimens containing PVA and MSP became more pronounced in contrast to those containing BS fiber and continued to decrease up to 800 °C.

3. There is a decrease occurs in the water absorption of the samples containing MSP fiber cured at 20 °C and not exposed to high-temperature effects. On the other hand, while the MSP samples were exposed to temperatures more than 200 °C, MSP fiber gradually melted and negatively affected the mechanical properties of the samples, since the melting point of MSP fiber is 165 °C. This study suggests using BS fiber for structures exposed to fire hazards, MSP fiber for structures exposed to water, and PVA fiber for structures requiring high energy absorption.

Declaration of Competing Interest

The authors wish to thank ARIE Research Group, CEU San Pablo University for the funds dedicated to the project ref. G20/6-06 Project: PENTALUZ: CECO: M02.0402 ORACLE: MPENTALU.

References

[1] R. Pierrehumbert, There is no Plan B for dealing with the climate crisis, Bull. At. Sci. 75 (5) (2019) 215–221.
[2] Mahmoud Ziada, Y. Tammam, S. Erdem, Research of alternative ecological waste materials used in geopolymers for sustainable built environments, in: R. A. González-Lezcano (Ed.), Urban Sustain. Energy Manag. Cities Improv. Heal. Well-Being, IGI Global, Hershey, PA, USA, 2022, pp. 159–178, 10.4018/978-1-6684-4030-8.ch009.
[3] M. Abdulkareem, J. Havukainen, M. Horttanainen, Environmental assessment of alkali-activated mortars using different activators. Proc. SARDINIA2019, 2019.
[4] V.F.F. Barbosa, K.J.D. MacKenzie, C. Thaumaturgo, Synthesis and characterisation of materials based on inorganic polymers of alumina and silica: Sodium polysialate polymers, Int. J. Inorg. Mater. 2 (2000) 309–317, https://doi.org/10.1016/S1466-6049(00)00041-6.
[5] M. Irfan Khan, H.U. Khan, K. Azizli, S. Sufian, Z. Man, A.A. Siyal, N. Muhammad, M. Faiz ur Rehman, The pyrolysis kinetics of the conversion of Malaysian kaolin to metakaolin, Appl. Clay Sci. 146 (2017) 152–161, https://doi.org/10.1016/j.clay.2017.05.017.
[6] H.K. Tchakouté, C.H. Rüscher, Mechanical and microstructural properties of metakaolin-based geopolymer cements from sodium waterglass and phosphoric acid solution as hardeners: A comparative study, Appl. Clay Sci. 140 (2017) 81–87.
[7] S. Tome, C.N. Bewa, A. Nana, J.G. Deutou Nemaleu, M.A. Etoh, H.K. Tchakouté, S. Kumar, J. Etame, Structural and physico-mechanical investigations of mine tailing-calcined kaolinite based phosphate geopolymer binder, Silicon 14 (2022) 3563–3570, https://doi.org/10.1007/s12633-021-01137-w.
[8] Z. Luo, Y. Ma, H. He, W. Mu, X. Zhou, W. Liao, H. Ma, Preparation and characterization of ferrous oxalate cement—A novel acid-base cement, J. Am. Ceram. Soc. 104 (2) (2021) 1120–1131.
[9] E.L. Foletto, G.C. Colazzo, C. Volzone, L.M. Porto, Sunflower oil bleaching by adsorption onto acid-activated bentonite, Brazilian, J Chem. Eng. 28 (1) (2011) 169–174.
[10] A. Mocciaro, M.S. Conconi, N.M. Rendtorff, A.N. Scian, Ceramic properties of kaolinitic clay with monoaluminum phosphate (Al(H2PO4)3) addition, J. Therm. Anal. Calorim. 144 (2021) 1083–1093, https://doi.org/10.1007/s10973-020-10488-2.
[11] S. Pu, Z. Zhu, W. Wang, W. Duan, Z. Wu, N. Li, P. Jiang, Water resistance of fly ash phosphoric acid-based geopolymer, Dev. Built Environ. 12 (2022), 100093, https://doi.org/10.1016/j.dibe.2022.100093.
[12] B. Gopalakrishna, P. Dinakar, Mix design development of fly ash-GGBS based recycled aggregate geopolymer concrete, J. Build. Eng. 63 (2023), 105551.

[13] Y. Luna-Galiano, C. Leiva, F. Arroyo, R. Villegas, L. Vilches, C. Fernández-Pereira, Development of fly ash-based geopolymers using powder sodium silicate activator, Mater. Lett. 320 (2022), 132346, https://doi.org/10.1016/j.matlet.2022.132346.
[14] M. Ziada, S. Erdem, Y. Tammam, S. Kara, R.A. Lezcano, The effect of basalt fiber on mechanical, microstructural, and high-temperature properties of fly ash-based and basalt powder waste-filled sustainable geopolymer mortar, Sustain. 13 (2021), https://doi.org/10.3390/su132212610.
[15] R. Somna, T. Saowapun, K. Somna, P. Chindaprasirt, Rice husk ash and fly ash geopolymer hollow block based on NaOH activated, Case Stud. Constr. Mater. 16 (2022) e01092.
[16] V. Trincal, S. Multon, V. Benavent, H. Lahalle, B. Balsamo, A. Caron, R. Bucher, L. Diaz Caselles, M. Cyr, Shrinkage mitigation of metakaolin-based geopolymer activated by sodium silicate solution, Cem. Concr. Res. 162 (2022), 106993, https://doi.org/10.1016/j.cemconres.2022.106993.
[17] E. Adesanya, K. Ohenoja, T. Luukkonen, P. Kinnunen, M. Illikainen, One-part geopolymer cement from slag and pretreated paper sludge, J. Clean. Prod. 185 (2018) 168–175, https://doi.org/10.1016/j.jclepro.2018.03.007.
[18] E. Adesanya, K. Ohenoja, P. Kinnunen, M. Illikainen, Properties and durability of alkali-activated ladle slag, Mater. Struct. 50 (2017) 255, https://doi.org/10.1617/s11527-017-1125-4.
[19] H. Maraghechi, S. Salwocki, F. Rajabipour, Utilisation of alkali activated glass powder in binary mixtures with Portland cement, slag, fly ash and hydrated lime, Mater. Struct. 50 (2016) 16, https://doi.org/10.1617/s11527-016-0922-5.
[20] Y. Tammam, M. Uysal, O. Canpolat, Ö.F. Kuranlı, Effect of waste filler materials and recycled waste aggregates on the production of geopolymer composites, Arab. J. Sci. Eng. (2022), https://doi.org/10.1007/s13369-022-07230-5.
[21] Y. Tammam, M. Uysal, O. Canpolat, Durability properties of fly ash-based geopolymer mortars with different quarry waste fillers, Comput. Concr. 29 (2022), https://doi.org/10.12989/cac.2022.29.5.335.
[22] K. Sagoe-Crentsil, T. Brown, A. Taylor, Drying shrinkage and creep performance of geopolymer concrete, J. Sustain. Cem. Mater. 2 (2013), https://doi.org/10.1080/21650373.2013.764963.
[23] S. Hu, H. Wang, G. Zhang, Q. Ding, Bonding and abrasion resistance of geopolymeric repair material made with steel slag, Cem. Concr. Compos. 30 (2008) 239–244, https://doi.org/10.1016/j.cemconcomp.2007.04.004.
[24] Z. Zhang, K. Wang, B. Mo, X. Li, X. Cui, Preparation and characterization of a reflective and heat insulative coating based on geopolymers, Energy Build. 87 (2015) 220–225, https://doi.org/10.1016/j.enbuild.2014.11.028.
[25] A.M. Rashad, A.S. Ouda, Thermal resistance of alkali-activated metakaolin pastes containing nano-silica particles, J. Therm. Anal. Calorim. 136 (2019) 609–620, https://doi.org/10.1007/s10973-018-7657-1.
[26] X. Jiang, R. Xiao, Y. Ma, M. Zhang, Y. Bai, B. Huang, Influence of waste glass powder on the physico-mechanical properties and microstructures of fly ash-based geopolymer paste after exposure to high temperatures, Constr. Build. Mater. 262 (2020), 120579, https://doi.org/10.1016/j.conbuildmat.2020.120579.
[27] K. Sakkas, A. Sofianos, P. Nomikos, D. Panias, Behaviour of passive fire protection K-geopolymer under successive severe fire incidents, Materials (Basel). 8 (2015) 6096–6104.
[28] H.M. Khater, M. Gharieb, Synergetic effect of nano-silica fume for enhancing physico-mechanical properties and thermal behavior of MK-geopolymer composites, Constr. Build. Mater. 350 (2022), 128879, https://doi.org/10.1016/j.conbuildmat.2022.128879.
[29] P. Duxson, J.L. Provis, G.C. Lukey, J.S.J. van Deventer, The role of inorganic polymer technology in the development of 'green concrete', Cem. Concr. Res. 37 (2007) 1590–1597, https://doi.org/10.1016/j.cemconres.2007.08.018.
[30] A. Autef, E. Joussein, G. Gasgnier, S. Pronier, I. Sobrados, J. Sanz, S. Rossignol, Role of metakaolin dehydroxylation in geopolymer synthesis, Powder Technol. 250 (2013) 33–39, https://doi.org/10.1016/j.powtec.2013.09.022.
[31] H. Wang, H. Li, F. Yan, Synthesis and mechanical properties of metakaolinite-based geopolymer, Colloids Surfaces A Physicochem. Eng. Asp. 268 (2005) 1–6, https://doi.org/10.1016/j.colsurfa.2005.01.016.
[32] J. Temuujin, W. Rickard, M. Lee, A. van Riessen, Preparation and thermal properties of fire resistant metakaolin-based geopolymer-type coatings, J. Non. Cryst. Solids. 357 (2011) 1399–1404, https://doi.org/10.1016/j.jnoncrysol.2010.09.063.
[33] J. Temuujin, A. Minjigmaa, W. Rickard, M. Lee, I. Williams, A. van Riessen, Fly ash based geopolymer thin coatings on metal substrates and its thermal evaluation, J. Hazard. Mater. 180 (2010) 748–752, https://doi.org/10.1016/j.jhazmat.2010.04.121.
[34] M. Mastali, P. Kinnunen, H. Isomoisio, M. Karhu, M. Illikainen, Mechanical and acoustic properties of fiber-reinforced alkali-activated slag foam concretes containing lightweight structural aggregates, Constr. Build. Mater. 187 (2018) 371–381, https://doi.org/10.1016/j.conbuildmat.2018.07.228.
[35] W.D.A. Rickard, L. Vickers, A. van Riessen, Performance of fibre reinforced, low density metakaolin geopolymers under simulated fire conditions, Appl. Clay Sci. 73 (2013) 71–77, https://doi.org/10.1016/j.clay.2012.10.006.
[36] W.-J. Long, H.-D. Li, L. Mei, W. Li, F. Xing, K.H. Khayat, Damping characteristics of PVA fiber-reinforced cementitious composite containing high-volume fly ash under frequency-temperature coupling effects, Cem. Concr. Compos. 118 (2021), 103911, https://doi.org/10.1016/j.cemconcomp.2020.103911.
[37] H. Wu, D. Zhang, B.R. Ellis, V.C. Li, Mechanical behavior of carbonated MgO-based Engineered Cementitious Composite (ECC) after high temperatures exposure, Cem. Concr. Compos. 124 (2021), 104255, https://doi.org/10.1016/j.cemconcomp.2021.104255.
[38] N. Hammad, A.M. ElNemr, H.-E.-D. Hassan, Flexural performance of reinforced Alkali-activated concrete beams incorporating steel and structural Macro synthetic polypropylene fiber, Constr. Build. Mater. 324 (2022), 126634, https://doi.org/10.1016/j.conbuildmat.2022.126634.
[39] M. Ziada, Y. Tammam, S. Erdem, R.A. Lezcano, Investigation of the mechanical, microstructure and 3D fractal analysis of nanocalcite-modified environmentally friendly and sustainable cementitious composites, Build. 12 (2022), https://doi.org/10.3390/buildings12010036.
[40] W.D.A. Rickard, G.J.G. Gluth, K. Pistol, In-situ thermo-mechanical testing of fly ash geopolymer concretes made with quartz and expanded clay aggregates, Cem. Concr. Res. 80 (2016) 33–43, https://doi.org/10.1016/j.cemconres.2015.11.006.
[41] Z. Pan, Z. Tao, Y.F. Cao, R. Wuhrer, T. Murphy, Compressive strength and microstructure of alkali-activated fly ash/slag binders at high temperature, Cem. Concr. Compos. 86 (2018) 9–18, https://doi.org/10.1016/j.cemconcomp.2017.09.011.
[42] P. Duxson, G.C. Lukey, J.S.J. van Deventer, Physical evolution of Na-geopolymer derived from metakaolin up to 1000 °C, J. Mater. Sci. 42 (2007) 3044–3054, https://doi.org/10.1007/s10853-006-0535-4.
[43] O.A. Abdulkareem, A.M. Mustafa Al Bakri, H. Kamarudin, I. Khairul Nizar, A. A. Saif, Effects of elevated temperatures on the thermal behavior and mechanical performance of fly ash geopolymer paste, mortar and lightweight concrete, Constr. Build. Mater. 50 (2014) 377–387.
[44] V. Lopresto, C. Leone, I. De Iorio, Mechanical characterisation of basalt fibre reinforced plastic, Compos. Part B Eng. 42 (2011) 717–723, https://doi.org/10.1016/j.compositesb.2011.01.030.
[45] J. Sim, C. Park, D.Y. Moon, Characteristics of basalt fiber as a strengthening material for concrete structures, Compos. Part B Eng. 36 (2005) 504–512, https://doi.org/10.1016/j.compositesb.2005.02.002.
[46] B. Wei, H. Cao, S. Song, Degradation of basalt fibre and glass fibre/epoxy resin composites in seawater, Corros. Sci. 53 (2011) 426–431, https://doi.org/10.1016/j.corsci.2010.09.053.
[47] W. Ahmed, C.W. Lim, Production of sustainable and structural fiber reinforced recycled aggregate concrete with improved fracture properties: A review, J. Clean. Prod. 279 (2021), 123832, https://doi.org/10.1016/j.jclepro.2020.123832.
[48] A.B. Kizilkanat, N. Kabay, V. Akyüncü, S. Chowdhury, A.H. Akça, Mechanical properties and fracture behavior of basalt and glass fiber reinforced concrete: An experimental study, Constr. Build. Mater. 100 (2015) 218–224, https://doi.org/10.1016/j.conbuildmat.2015.10.006.
[49] X. Sun, Z. Gao, P. Cao, C. Zhou, Mechanical properties tests and multiscale numerical simulations for basalt fiber reinforced concrete, Constr. Build. Mater. 202 (2019) 58–72, https://doi.org/10.1016/j.conbuildmat.2019.01.018.
[50] V. Chernov, H. Zlotnikov, M. Shandalov, Structural synthetic fiber-reinforced concrete, Concr. Int. 28 (2006) 56–61.
[51] S.H. Diab, A.M. Soliman, M. Nokken, Performance-based design for fiber-reinforced concrete: Potential balancing corrosion risk and strength, J. Mater. Civ. Eng. 32 (2020) 4019362.
[52] V. Guerini, A. Conforti, G. Plizzari, S. Kawashima, Influence of steel and macro-synthetic fibers on concrete properties, Fibers. 6 (2018), https://doi.org/10.3390/fib6030047.
[53] M.N.S. Hadi, Using fibres to enhance the properties of concrete columns, Constr. Build. Mater. 21 (2007) 118–125, https://doi.org/10.1016/j.conbuildmat.2005.06.028.
[54] K. Dhasindrakrishna, K. Pasupathy, S. Ramakrishnan, J. Sanjayan, Rheology and elevated temperature performance of geopolymer foam concrete with varying PVA fibre dosage, Mater. Lett. 328 (2022), 133122, https://doi.org/10.1016/j.matlet.2022.133122.
[55] Y. Haddaji, H. Majdoubi, S. Mansouri, T.S. Alomayri, D. Allaoui, B. Manoun, M. Oumam, H. Hannache, Microstructure and flexural performances of glass fibers reinforced phosphate sludge based geopolymers at elevated temperatures, Case Stud. Constr. Mater. 16 (2022) e00928.
[56] P. Zhang, X. Han, S. Hu, J. Wang, T. Wang, High-temperature behavior of polyvinyl alcohol fiber-reinforced metakaolin/fly ash-based geopolymer mortar, Compos. Part B Eng. 244 (2022), 110171, https://doi.org/10.1016/j.compositesb.2022.110171.
[57] H. Tanyildizi, M. Ziada, M. Uysal, N. Doğruöz Güngör, A. Coşkun, Comparison of bacteria-based self-healing methods in metakaolin geopolymer mortars, Case Stud. Constr. Mater. (2022), https://doi.org/10.1016/j.cscm.2022.e00895 e00895.
[58] M. Ziada, H. Tanyildizi, M. Uysal, Bacterial healing of geopolymer concrete exposed to combined sulfate and freeze-thaw effects, Constr. Build. Mater. 369 (2023), 130517, https://doi.org/10.1016/j.conbuildmat.2023.130517.
[59] R.t.c., 200-HTC, Recommendation of RILEM TC 200-HTC: mechanical concrete properties at high temperatures—modelling and applications, Mater. Struct. 40 (2007) 841–853, https://doi.org/10.1617/s11527-007-9285-2.
[60] Y. Ling, P. Zhang, J. Wang, Y. Chen, Effect of PVA fiber on mechanical properties of cementitious composite with and without nano-SiO2, Constr. Build. Mater. 229 (2019), 117068, https://doi.org/10.1016/j.conbuildmat.2019.117068.
[61] S. Xu, M.A. Malik, Z. Qi, B. Huang, Q. Li, M. Sarkar, Influence of the PVA fibers and SiO2 NPs on the structural properties of fly ash based sustainable geopolymer, Constr. Build. Mater. 164 (2018) 238–245, https://doi.org/10.1016/j.conbuildmat.2017.12.227.
[62] J. Topič, Z. Prošek, K. Indrová, T. Plachý, V. Nežerka, L. Kopecky, P. Tesarek, Effect of PVA modification on the properties of cement composites, Acta Polytech. 55 (2015) 64–75, https://doi.org/10.14311/AP.2015.55.0064.
[63] D.V. Soulioti, N.M. Barkoula, A. Paipetis, T.E. Matikas, Effects of fibre geometry and volume fraction on the flexural behaviour of steel-fibre reinforced concrete, Strain 47 (2011) e535–e541.

[64] H. Katkhuda, N. Shatarat, Improving the mechanical properties of recycled concrete aggregate using chopped basalt fibers and acid treatment, Constr. Build. Mater. 140 (2017) 328–335, https://doi.org/10.1016/j.conbuildmat.2017.02.128.
[65] M. Hassani Niaki, A. Fereidoon, M. Ghorbanzadeh Ahangari, Experimental study on the mechanical and thermal properties of basalt fiber and nanoclay reinforced polymer concrete, Compos. Struct. 191 (2018) 231–238, https://doi.org/10.1016/j.compstruct.2018.02.063.
[66] C. Jiang, K. Fan, F. Wu, D. Chen, Experimental study on the mechanical properties and microstructure of chopped basalt fibre reinforced concrete, Mater. Des. 58 (2014) 187–193, https://doi.org/10.1016/j.matdes.2014.01.056.
[67] N. Yousefieh, A. Joshaghani, E. Hajibandeh, M. Shekarchi, Influence of fibers on drying shrinkage in restrained concrete, Constr. Build. Mater. 148 (2017) 833–845, https://doi.org/10.1016/j.conbuildmat.2017.05.093.
[68] H. Mohammadhosseini, A.S.M. Abdul Awal, J.B. Mohd Yatim, The impact resistance and mechanical properties of concrete reinforced with waste polypropylene carpet fibres, Constr. Build. Mater. 143 (2017) 147–157, https://doi.org/10.1016/j.conbuildmat.2017.03.109.
[69] O. Karahan, C.D. Atiş, The durability properties of polypropylene fiber reinforced fly ash concrete, Mater. Des. 32 (2011) 1044–1049, https://doi.org/10.1016/j.matdes.2010.07.011.
[70] T. Yaowarat, S. Horpibulsuk, A. Arulrajah, M. Mirzababaei, A.S.A. Rashid, Compressive and flexural strength of polyvinyl alcohol–modified pavement concrete using recycled concrete aggregates, J. Mater. Civ. Eng. 30 (2018) 4018046.
[71] S.F.U. Ahmed, H. Mihashi, Strain hardening behavior of lightweight hybrid polyvinyl alcohol (PVA) fiber reinforced cement composites, Mater. Struct. 44 (2011) 1179–1191, https://doi.org/10.1617/s11527-010-9691-8.
[72] A. Akkari, Evaluation of a Polyvinyl Alcohol Fiber Reinforced Engineered Cementitious Composite For A Thin-Bonded Pavement Overlay, Minnesota Department of Transportation, Research Services Section, 2011.
[73] N. Kabay, Abrasion resistance and fracture energy of concretes with basalt fiber, Constr. Build. Mater. 50 (2014) 95–101, https://doi.org/10.1016/j.conbuildmat.2013.09.040.
[74] R. Abaeian, H.P. Behbahani, S.J. Moslem, Effects of high temperatures on mechanical behavior of high strength concrete reinforced with high performance synthetic macro polypropylene (HPP) fibres, Constr. Build. Mater. 165 (2018) 631–638, https://doi.org/10.1016/j.conbuildmat.2018.01.064.
[75] K.D. Joo, W. Kay, E.-T. Sherif, N.A. E., Testing of cementitious materials under high-strain-rate tensile loading using elastic strain energy, J. Eng. Mech. 137 (2011) 268–275, https://doi.org/10.1061/(ASCE)EM.1943-7889.0000224.
[76] Y. Ma, B. Zhu, M. Tan, Properties of ceramic fiber reinforced cement composites, Cem. Concr. Res. 35 (2005) 296–300, https://doi.org/10.1016/j.cemconres.2004.05.017.
[77] C. Lu, J. Yu, C.K.Y. Leung, Tensile performance and impact resistance of Strain Hardening Cementitious Composites (SHCC) with recycled fibers, Constr. Build. Mater. 171 (2018) 566–576, https://doi.org/10.1016/j.conbuildmat.2018.03.108.
[78] V. Afroughsabet, T. Ozbakkaloglu, Mechanical and durability properties of high-strength concrete containing steel and polypropylene fibers, Constr. Build. Mater. 94 (2015) 73–82, https://doi.org/10.1016/j.conbuildmat.2015.06.051.
[79] Z. Abdollahnejad, M. Mastali, T. Luukkonen, P. Kinnunen, M. Illikainen, Fiber-reinforced one-part alkali-activated slag/ceramic binders, Ceram. Int. 44 (2018) 8963–8976, https://doi.org/10.1016/j.ceramint.2018.02.097.
[80] S.F.A. Shah, B. Chen, S.Y. Oderji, M. Aminul Haque, M.R. Ahmad, Comparative study on the effect of fiber type and content on the performance of one-part alkali-activated mortar, Constr. Build. Mater. 243 (2020), 118221, https://doi.org/10.1016/j.conbuildmat.2020.118221.
[81] A. Sadrmomtazi, B. Tahmouresi, A. Saradar, Effects of silica fume on mechanical strength and microstructure of basalt fiber reinforced cementitious composites (BFRCC), Constr. Build. Mater. 162 (2018) 321–333, https://doi.org/10.1016/j.conbuildmat.2017.11.159.
[82] K. Behfarnia, A. Behravan, Application of high performance polypropylene fibers in concrete lining of water tunnels, Mater. Des. 55 (2014) 274–279, https://doi.org/10.1016/j.matdes.2013.09.075.
[83] H. Bolat, O. Şimşek, M. Çullu, G. Durmuş, Ö. Can, The effects of macro synthetic fiber reinforcement use on physical and mechanical properties of concrete, Compos. Part B Eng. 61 (2014) 191–198, https://doi.org/10.1016/j.compositesb.2014.01.043.
[84] A. Saradar, P. Nemati, A.S. Paskiabi, M.M. Moein, H. Moez, E.H. Vishki, Prediction of mechanical properties of lightweight basalt fiber reinforced concrete containing silica fume and fly ash: Experimental and numerical assessment, J. Build. Eng. 32 (2020), 101732, https://doi.org/10.1016/j.jobe.2020.101732.
[85] H. Dilbas, Ö. Çakır, Influence of basalt fiber on physical and mechanical properties of treated recycled aggregate concrete, Constr. Build. Mater. 254 (2020), 119216, https://doi.org/10.1016/j.conbuildmat.2020.119216.
[86] Y. Tammam, M. Uysal, O. Canpolat, Effects of alternative ecological fillers on the mechanical, durability, and microstructure of fly ash-based geopolymer mortar, Eur. J. Environ. Civ. Eng. (2021) 1–24, https://doi.org/10.1080/19648189.2021.1925157.
[87] N. Balgourinejad, M. Haghighifar, R. Madandoust, S. Charkhtab, Experimental study on mechanical properties, microstructural of lightweight concrete incorporating polypropylene fibers and metakaolin at high temperatures, J. Mater. Res. Technol. 18 (2022) 5238–5256, https://doi.org/10.1016/j.jmrt.2022.04.005.
[88] B. Nematollahi, J. Sanjayan, F.U.A. Shaikh, Comparative deflection hardening behavior of short fiber reinforced geopolymer composites, Constr. Build. Mater. 70 (2014) 54–64, https://doi.org/10.1016/j.conbuildmat.2014.07.085.
[89] K. Zerfu, J.J. Ekaputri, Bond strength in PVA fibre reinforced fly ash-based geopolymer concrete, Mag. Civ. Eng. 101 (2021).
[90] J. Alves, A. El-Ragaby, E. El-Salakawy, Durability of GFRP bars' bond to concrete under different loading and environmental conditions, J. Compos. Constr. 15 (3) (2011) 249–262.
[91] K.M.A. Hossain, D. Ametrano, M. Lachemi, Bond strength of standard and high-modulus GFRP bars in high-strength concrete, J. Mater. Civ. Eng. 26 (3) (2014) 449–456.
[92] A. Adesina, Performance of cementitious composites reinforced with chopped basalt fibres – An overview, Constr. Build. Mater. 266 (2021), 120970, https://doi.org/10.1016/j.conbuildmat.2020.120970.
[93] H.Y. Zhang, V. Kodur, B. Wu, L. Cao, S.L. Qi, Comparative thermal and mechanical performance of geopolymers derived from metakaolin and fly ash, J. Mater. Civ. Eng. 28 (2016) 4015092.
[94] X. Jiang, R. Xiao, M. Zhang, W. Hu, Y. Bai, B. Huang, A laboratory investigation of steel to fly ash-based geopolymer paste bonding behavior after exposure to elevated temperatures, Constr. Build. Mater. 254 (2020), 119267, https://doi.org/10.1016/j.conbuildmat.2020.119267.
[95] J. Xu, A. Kang, Z. Wu, P. Xiao, Y. Gong, Effect of high-calcium basalt fiber on the workability, mechanical properties and microstructure of slag-fly ash geopolymer grouting material, Constr. Build. Mater. 302 (2021), 124089, https://doi.org/10.1016/j.conbuildmat.2021.124089.
[96] M. Afroz, I. Patnaikuni, S. Venkatesan, Chemical durability and performance of modified basalt fiber in concrete medium, Constr. Build. Mater. 154 (2017) 191–203, https://doi.org/10.1016/j.conbuildmat.2017.07.153.